

# Turbidity Reduction of Groundwater by Using Nanomagnetic Adsorbent Composite

## (NMAC): Process Optimization by 3<sup>k</sup> Factorial Design and Analysis

Huda Awang<sup>1</sup>, Nor Asfaliza Abdullah<sup>1</sup>, Jayanthi Barasarathi.<sup>2</sup>, Ho Yoon Ling <sup>1</sup>, Lim Kai Wen <sup>1</sup>,  
Hanis Nadhirah<sup>1</sup>, Siti Nuurul Huda Mohammad Azmin<sup>1</sup>, Palsan Sannasi Abdullah<sup>1,\*</sup>

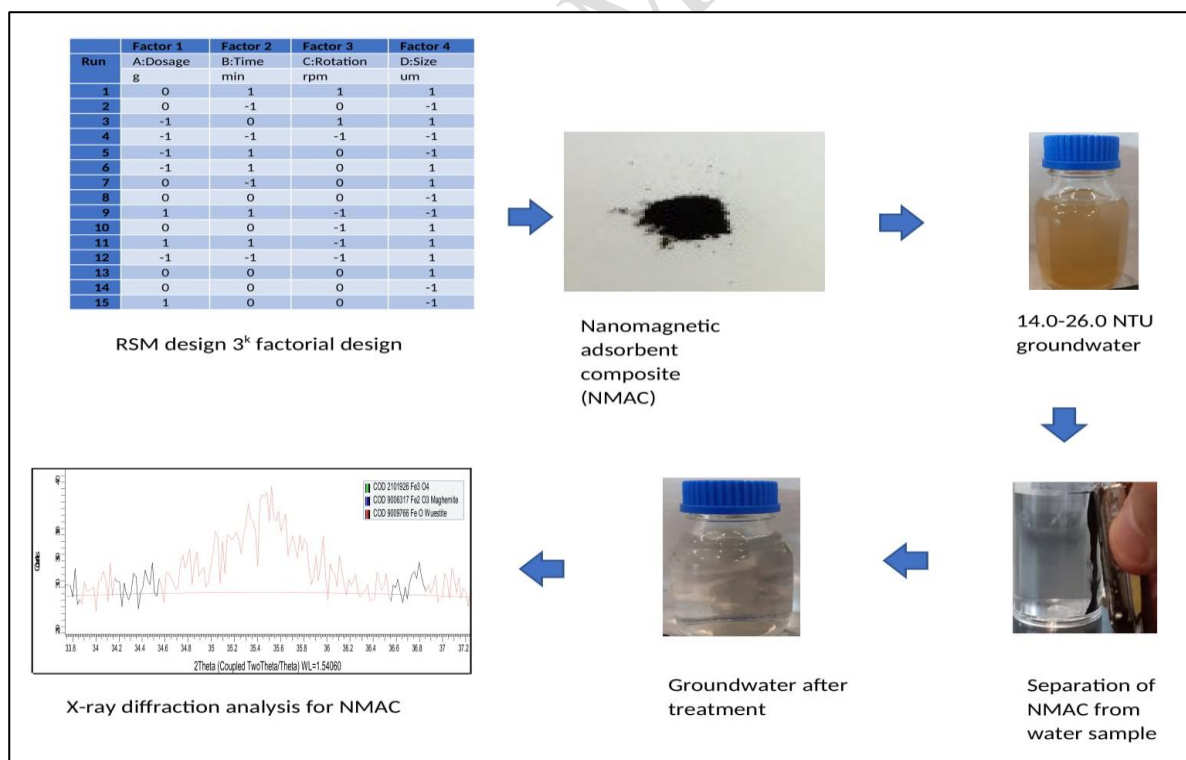
<sup>1</sup> Faculty of Agro-Based Industry, Universiti Malaysia Kelantan Jeli Campus 17600 Jeli, Kelantan,  
Malaysia

<sup>2</sup> Faculty of Health and Life Sciences, Inti International University, Nilai, Negeri Sembilan, Malaysia

\*Corresponding author:

E-mail: ([palsan.abdullah@umk.edu.my](mailto:palsan.abdullah@umk.edu.my)), tel: +6099477444

### GRAPHICAL ABSTRACT



12

13

14

## 15 ABSTRACT

16 The widespread use of alternative water sources in Kelantan encourages the development of cost-  
17 effective methods for the purification of water. A simple and straightforward adsorption process using  
18 a nanomagnetic adsorption composite (NMAC) was introduced in this study as a new adsorbent for  
19 the treatment of turbid polluted groundwater. The use of iron oxide nano-coated adsorbents (NMACs)  
20 showed a high porosity relative to commercial activated carbons (CACs). Analysis of X-ray  
21 diffraction analysis for NMAC is confirmed by a crystal framework for  $\text{Fe}_2\text{O}_3$ ,  $\text{Fe}_3\text{O}_4$ , and  $\text{FeO}$  are  
22 cubic components. A  $3^k$  maximum factor configuration of four factors, i.e., adsorbent dosage (0.02,  
23 0.04, and 0.06 g), agitation time (15, 30, and 60 min), rotation speed (150, 200, and 250 rpm) and  
24 adsorbent scale ( $< 45 \mu\text{m}$  and  $> 300 \mu\text{m}$ ) were used. The turbidity removal capability of both NMAC  
25 and CAC was compared. The adequacy of the developed empirical model for the elimination of  
26 turbidity and maximum turbidity efficiency was determined by regression model analysis. The  
27 obtained results revealed regression values of NMAC ( $R^2$ ; 0.9903,  $R^2$  adj.; 0.9875,  $R^2$  pred; 0.9808)  
28 and CAC ( $R^2$ ; 0.9909,  $R^2$  adj.; 0.9981,  $R^2$  pred.; 0.9817). The analysis of variance and surface  
29 response methodology revealed that turbidity removal efficiency of NMAC is affected by the four  
30 factors investigated. Among the samples, 0.04 g NMAC ( $< 45 \mu\text{m}$ ) agitated at 150 rpm for 48 min  
31 showed 98.76% maximum adsorption efficiency. The findings showed that NMAC is a strong  
32 adsorbent for use in the treatment of raw water.

33 **Keywords:** Activated carbon, adsorbent, factorial design, nanomagnetic composite, turbidity,  
34 wastewater

## 35 1. Introduction

36 The use of groundwater is still common among Malaysians, especially at east coast of peninsular  
37 Malaysia, Kelantan and about 38% of the population in the State of Kelantan use groundwater for  
38 consumption (Ayob et al, 2022). Residents in the northern part of Kelantan are taking advantage of  
39 the aquifer for consuming groundwater at a high rate ( $4.22 \pm 0.17 \text{ mm/year}$ ) (Yong *et al.*, 2018). The

40 rapid growth of the population and accelerated urbanization raises demand for groundwater  
41 consumption. Groundwater provides half of all water used by households worldwide, a quarter of all  
42 the water drawn for irrigated agriculture, and one third of the water supply required for industry  
43 (WHO, 2022). Improper disposal of wastewater coming from municipal and agricultural sources with  
44 little to no treatment before discharge is considered a common practice, and this has led to the eventual  
45 leaching of contaminants into the soil, which causes the significant depletion of groundwater quality  
46 (Zainol et al., 2021) and furthermore improper waste management among industry operators and  
47 excavation that exceeds the groundwater aquifer level leads to turbidity problem with groundwater  
48 (Mohd Faiz & Noorazuan, 2018). A preliminary study conducted at Tanah Merah, Pasir Mas, and  
49 Jeli revealed that turbidity reading ( $>5$  NTU) of samples from tube well exceeded the Drinking Water  
50 Quality Standard (Minister of Health, 2012; Huda et al., 2020; Huda et al., 2022). There are different  
51 methods applied to overcome the problem, including coagulation, flocculation, and membrane  
52 filtration (Park *et al.*, 2020). The formation of turbidity in water is due to the decomposition of organic  
53 matter by soil microorganisms known as humus, and the presence of peat soil with high iron content  
54 (Hazimah *et al.*, 2019). The presence of turbidity in groundwater not only reduces the aesthetic quality  
55 of the water but is also associated with gastrointestinal acid reflux disease among consumers (Muoio  
56 *et al.*, 2020). The use of poly aluminum chloride (PAC) coagulant is able to decrease residual  
57 turbidity to below 1.0 NTU. However, the drawback of coagulation is the removal of dissolved  
58 organic matter (Liu *et al.*, 2018). Adsorption is one of the more preferred conventional cleanup  
59 methods applied by industries for water treatment. Adsorption has commonly been opted for water  
60 treatment not only due to its simplicity but also for its performance. The adsorption process most  
61 likely involves physical rather than chemical phenomenon because a stable molecular surface  
62 complex will form at the interface during adsorption (Crini *et al.*, 2018). Powdered activated carbon  
63 (PAC) is widely used as adsorbent due to its high surface area and adsorption capacity. However, the  
64 recovery process for the spent powdered activated carbon through a gravitational separation is  
65 challenging due to small particle size, therefore increasing costs for treatment (Meng *et al.*, 2019).

66 Iron oxide nanomaterial called hematite ( $\alpha$ -Fe<sub>2</sub>O<sub>3</sub>) is magnetic, with lower operation costs, higher  
67 adsorption property, and environmentally friendly (Santosh *et al.*, 2019). Although hematite ( $\alpha$ -  
68 Fe<sub>2</sub>O<sub>3</sub>) particles self-aggregate during adsorption, modification of its surface by anchoring the  
69 particles onto organic molecules can overcome the problem (Tancredi *et al.*, 2019). The innovation  
70 had been done by tailoring the iron oxide nanoparticles on powdered activated carbon known as  
71 nanomagnetic adsorbent composite (NMAC). The adsorption of copper (Cu<sup>2+</sup>) by NMAC showed  
72 88% removal efficiency (Wannahari *et al.*, 2018). Therefore, the innovation improves not only  
73 adsorption activity but also the recovery of the NMAC from solution by applying an external  
74 magnetic field (Wannahari *et al.*, 2018). However, the NMAC efficiency in removing turbidity from  
75 raw water has not been tested yet. It is critical to remove turbidity in groundwater with Malaysia  
76 Drinking Water Standard (below 5 NTU) compliance. Apart of that, application of agricultural waste  
77 as source for biodegradable adsorbent is getting attention among researchers due to potential of  
78 competing commercial activated carbon (Basrur & Ishwara, 2019). Thus, agricultural waste was  
79 utilized to develop adsorbent components for NMAC (Wannahari *et al.*, 2018). The addressed  
80 challenges for NMAC include recovering the NMAC in the separation process and competing for  
81 commercial activated carbon (CAC). Therefore, the optimization of NMAC adsorption was  
82 conducted by adopting a 3<sup>k</sup> factorial design. Four factors were considered, including dosage of  
83 adsorbent, size of adsorbent, rotation speed, and time for agitation with three levels for each factor.  
84 In this study, significant factors and interactions were identified, while the optimum levels of the  
85 variables increase removal efficiency.

## 86 **2. Materials and methods**

### 87 *2.1. Chemicals*

88 All reagents used for the iodine number tests are of analytical grade. An iodine solution (0.1 N) was  
89 prepared from iodine pearl (Friendemann Schmidt Chemical) and potassium iodide (KI; Friendemann  
90 Schmidt Chemical) with iodine-to-iodide weight ratio 1:1.5. A 0.1 N sodium thiosulphate

91 pentahydrate ( $\text{Na}_2\text{S}_2\text{O}_3 \cdot 5\text{H}_2\text{O}$ ; Friendemann Schmidt Chemical) was prepared with 0.1 g sodium  
92 carbonate ( $\text{Na}_2\text{CO}_3$ ). A 10 % starch solution was used during titration.

## 93 2.2. Preparation and characterization of adsorbate

94 All of NMAC preparation steps were adapted from Wannahari et al.,(2018). To begin with, coconut  
95 shell (CS) went through pyrolysis process to produce powdered carbonized CS prior to potassium  
96 hydroxide (KOH) activation process with slow agitation for 5 to 6 h . Then, the activated coconut  
97 shell (ACS) was filtered, rinsed with distilled water, and dried in an oven at 100 °C. Later, the sample  
98 continued drying process in a muffle furnace (Carbolite ELF 11/6B) at range 800-900 °C with rate  
99 (10 °C/min). The dried sample was cooled down for 30 minutes before washing and treating with  
100 5% HCl. The treated ACS sample was dried again in an oven 100 °C and treated with nitric acid  
101 ( $\text{HNO}_3$ ) solution for 1 h at 80 °C.

102 Reaction solution was prepared by using mechanical stirring for dissolving  $\text{FeCl}_3 \cdot 6\text{H}_2\text{O}$  and  
103  $\text{FeSO}_4 \cdot 7\text{H}_2\text{O}$  in 450 mL of deionized water for 30 min at 30 °C. Next, 30-60 mL of ammonium  
104 hydroxide ( $\text{NH}_3 \cdot \text{H}_2\text{O}$ ) solution was mixed vigorously at 70 °C for 1 h to form precipitate. Later, 5 g  
105 of the prepared ACS sample in previous stage was mixed into the reaction solution followed by  
106 addition of 6 mL epichlorohydrin and continued stirring process at 85 °C for 1 h. Sonication (Q  
107 sonica) of reaction mixture took place at 80  $\lambda$  for 1 h by using. Upon completion of sonication, stirring  
108 process was continued for 1h at 85 °C. Then, the synthesized NMAC was cooled down at 27° C,  
109 washed with deionized water and ethanol, test for pH and dried for 48 h at 50 °C. The NMAC was  
110 sieved accordingly (<45  $\mu\text{m}$ ) and (>300  $\mu\text{m}$ ) and ready for application.

111 The CAC was also washed, neutralized, dried, and sieved accordingly.

### 112 2.2.1. Proximate analysis

113 Proximate analysis to determine the volatile matter, moisture, ash, and fixed carbon content of the  
114 respective adsorbate was conducted as per procedure (Milne *et al.*, 1992). The iodine number  
115 determination was carried out by adopting the standard method for activated carbon (ASTM, 2006).

116 2.2.2. *Surface characterization of NMAC*

117 The Brunauer-Emmett-Teller (BET) analysis was performed to identify total pore volume (m<sup>3</sup>/g),  
118 average pore volume (nm), and BET surface area (m<sup>2</sup>/g) by using a Quantachrome Autosorb iQ3  
119 Automated Gas Sorption Analyzer (Quantachrome Instruments, US) at 77K. Analysis of crystalline  
120 structures (iron oxide nanomaterials) of NMAC was carried out through X-ray diffraction analysis  
121 (XRD; Bruker, D8 Advance X-RD) aided by Diffract Plus Eva Software for crystalline state  
122 detection. The analyses were conducted at room temperature with the following conditions; uncoated  
123 samples used, CuK $\alpha$  radiation ( $\lambda = 1.5406 \text{ \AA}$ ) in the 0.01% s range started at 2 $\theta$ : 5° to 90°.  
124 Measurement for the size of particle was carried out in a Zetasizer nano series ver. 7.03 (Malvern  
125 Ltd). Meanwhile, observation for morphology and elemental analysis was performed through JEOL  
126 SEM/EDX (JSM 6400) instrument with 15 kV.

127 2.3. *Water sampling*

128 The turbid groundwater was taken from a local well in Tanah Merah, Kelantan (coordinates: N 5°  
129 4856.8 E 102°0757.1. The initial turbidity of this raw water was approximately 23NTU.

130 2.4. *Batch adsorption studies*

131 The adsorption study was conducted by batch method with 10% adsorbent in the working volume.  
132 The parameters tested for the adsorption were the size of adsorbent, dosage of adsorbent, rotation  
133 speed, and time of agitation. The test adsorbent was NMAC, while CAC was the reference. The  
134 percentage of turbidity removal was calculated as in Eq. 1.

135 
$$\text{Percentage of turbidity removal} = \frac{NTU_i - NTU_e}{NTU_i} \times 100 \dots\dots\dots \text{Equation 1}$$

136 NTU<sub>i</sub> = Initial NTU reading

137 NTU<sub>e</sub> = Residual NTU reading at equilibrium

138 2.4. *Analytical method for groundwater sample*

139 The turbidity of groundwater was measured by using turbidity meter with a fast tracker (Hanna  
140 Instruments, Romania).

#### 141 2.5. Statistical analysis

142 In order to study the removal of turbidity responses to variation in parameters, the 3-Factorial design  
143 is used by the application of Response Surface Methodology (RSM) approach. The strategies in this  
144 method are; design of experiments (DOE) to evaluate model parameters after conducting experiments  
145 and develop second-order polynomial (Eq. 2) based on the obtained responses (Tezcan *et al.*, 2015).

$$146 \quad y = \beta_0 + \sum_{i=1}^k \beta_{ij}x_i + \sum_{i=1}^k \beta_{ij}x_i^2 + \sum_{i < j=2}^k \sum_{i=1}^k \beta_{ij}x_i x_j + \varepsilon$$

147  
148 (Equation 2)

149 The equation consisted of predicted response ( $y$ ), the number of factors ( $k$ ), constant ( $\beta_0$ ),  $i$ th linear  
150 coefficient ( $\beta_i$ ),  $i$ th quadratic coefficient ( $\beta_{ij}$ ),  $i$ th interaction coefficient ( $\beta_{ij}$ ), the independent variable  
151 ( $x_i$ ), and error ( $\varepsilon$ ).

152 In this study, the 3k factorial design for numerical factors consisted of dosage, agitation time, and  
153 rotation speed denoted as A, B, and C. Meanwhile the categorical factor involved the size of the  
154 adsorbent denoted as D. The levels of each factor were coded as -1 (low), 0 (middle), and 1 (high) as  
155 in Table 1.

156 **Table 1.** Input factors for 3k factorial design and their levels.

Types of factors	Factors	Unit	Symbol	Levels		
				-1	0	1
Numerical	Dosage adsorbent	of g	A	0.02	0.04	0.06
	Time of agitation	min	B	15	30	60
	Rotation speed	rpm	C	150	200	250

Categorical	Size of adsorbent	$\mu\text{m}$	D	< 45	>_300
-------------	-------------------	---------------	---	------	-------

157

158

159 Numerical considerations differed with an additional six center points on 27 different treatments, so  
 160 cumulative runs totaled to 33 (n=33). Since the design involves a two-level categorical element, this  
 161 experiment was duplicated with up to 66 total runs (n=66). The percentage of removal efficiency was  
 162 used as response of treatments combinations. An empirical model was generated after handling the  
 163 response of each combination. The calculation of fitting values and checking the adequacy of the  
 164 model, was carried out. The analysis of variance (ANOVA) for each factor was adopted by using  
 165 Design Expert ver. 11. An optimization with verification process was conducted to test the reliability  
 166 of the generated empirical model.

### 167 3. Results and Discussion

#### 168 3.1. Characterization of adsorbent composites

##### 169 3.1.1. Proximate analyses

170 The results of proximate analyses (Table 2) show that NMAC possesses higher moisture content, ash  
 171 content, and fixed carbon compared to CAC. The moisture content of NMAC is higher than CAC  
 172 because of the moisture adsorbing nature of the carbonate group, and the iron oxide nanoparticles  
 173 found in NMAC pores; a similar finding reported by Karthikeyan *et al.*, (2008). Ash contents are  
 174 minerals residue such as magnesium, calcium, and sodium in the pore of activated carbon (Zulkarnia  
 175 *et al.*, 2018). NMAC has higher ash contents in comparison to CAC, so it is undesirable as it might  
 176 reduce the mechanical strength of carbon for adsorption (Hidayu *et al.*, 2013). Besides, a low  
 177 percentage of volatile matter indicates that the pore structure of NMAC is porous and rigid as opposed  
 178 to CAC (Hidayu *et al.*, 2013). Iodine number test was conducted to identify the porosity of the  
 179 adsorbent. The BET analysis showed total pore volume, BET surface, and average pore volume of  
 180 NMAC were 0.67 m<sup>3</sup>/g, 916.19 m<sup>2</sup>/g, and 14.6 nm compared to CAC (0.46 m<sup>3</sup>/g, 769.50 m<sup>2</sup>/g, and  
 181 20.53 nm). Based on the obtained result, the porosity of NMAC is higher than CAC. The presence of



182 iron oxide nanomaterial increases the porosity of NMAC. Therefore, NMAC can be an efficient  
183 adsorbent in terms of surface areas, and pore volumes of porous material are vital factors for high-  
184 performance adsorption (Sun *et al.*, 2019).

185 **Table 2.** Comparison of proximate analysis between NMAC and CAC.

Parameter	NMAC	CAC
Moisture content (%)	3.71	2.75
Ash content (%)	22.96	20.27
Volatile (%)	13.52	19.77
Fixed carbon (%)	59.81	57.10
Iodine number	913.50	869.10

186

### 187 3.1.1. Characterization of nanomagnetic adsorbent composite (NMAC)

188 Iron oxide nanomaterials not only increase porosity but also contribute to magnetic property on the  
189 adsorbent. The presence of Fe<sub>2</sub>O<sub>3</sub>, Fe<sub>3</sub>O<sub>4</sub>, and FeO in the diffraction peaks characteristics of XRD  
190 patterns indicate the existence of magnetic microcrystalline on NMAC. The spectrum reading  
191 determined the presence of Fe<sub>2</sub>O<sub>3</sub>, Fe<sub>3</sub>O<sub>4</sub>, and FeO by peak observed at 35.522°, 35.721°, and 35.928°,  
192 respectively. Based on the analysis, as in Figure 1, the crystalline system structure of the composite  
193 is cubic. The present findings seem to agree with another research by Zhu (2018) reveals that the  
194 occurrence of nanomagnetic particles for peaks at 2θ (Fe<sub>3</sub>O<sub>4</sub>) are 30.22°, 35.62°, 57.50° and 62.42°  
195 which was used for the synthesis of bamboo biochar coated with α-Fe<sub>2</sub>O<sub>3</sub> / Fe<sub>3</sub>O<sub>3</sub> through  
196 impregnation of ferric solution.

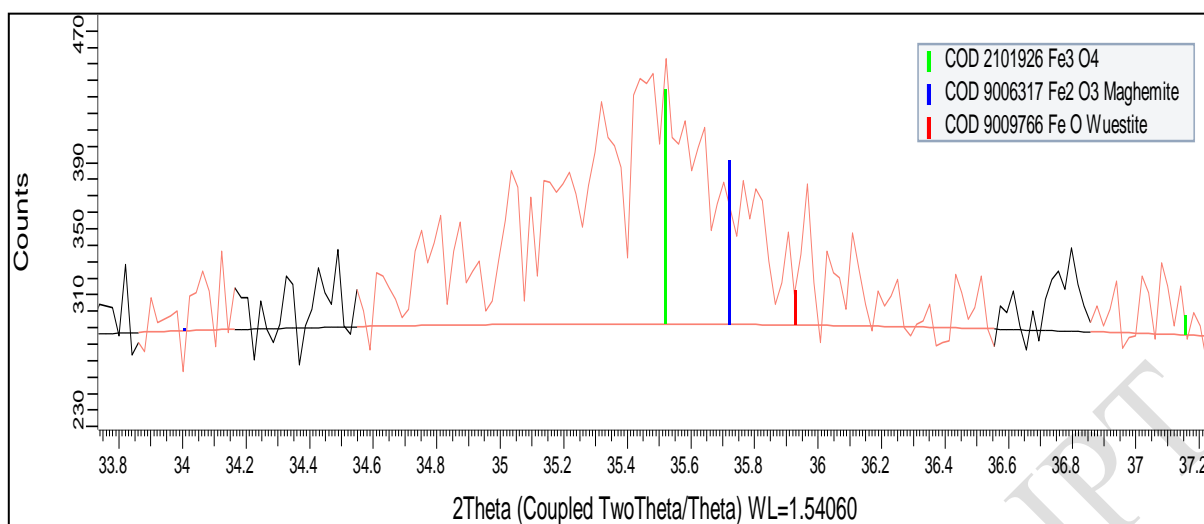


**Figure 1.** Intense peaks that indicated the presence of  $\text{Fe}_2\text{O}_3$ ,  $\text{Fe}_3\text{O}_4$ , and  $\text{FeO}$  at  $2\theta$  peaks of  $35.522^\circ$ ,  $35.721^\circ$ , and  $35.928^\circ$  respectively.

197  
198  
199  
200

### 201 3.2. Adsorption study of the nanomagnetic adsorbent composite (NMAC)

202 The design matrix (codified value) and the response value for the percentage of turbidity removal are  
 203 shown in Table 3. The results showed that NMAC with a particle size less (<) than  $45\ \mu\text{m}$  is favorable  
 204 for the removal of turbidity, whereas CAC with a size greater (>) than  $300\ \mu\text{m}$  was better for the  
 205 removal of turbidity. It might be due to the efficiency of the separation process. Despite their small  
 206 size, NMAC particles were separated completely during the turbidity test without contaminating  
 207 recovered water samples. Although Table 3 was not being considered as the response of the full  
 208 factorial design, it is important to note that the minimum turbidity removal efficiency by NMAC is  
 209  $84.54\%$  (  $0.02\ \text{g}$  NMAC, 15 mins, 150 rpm, and size of adsorbent  $>300\ \mu\text{m}$ ) which was higher when  
 210 compared to minimum value resulted by CAC ( $65.96\%$ ) with  $0.02\ \text{g}$  CAC, 60 mins, 200 rpm, and  
 211  $<45\ \mu\text{m}$  of adsorbent. The NMAC adsorption results of this study are similar to Kim (2013) findings,  
 212 which used iron oxide nanoparticles-impregnated powder activated carbon (IPAC) to remove organic  
 213 matter from raw water, resulting in a removal efficiency of more than  $80\%$ . Therefore, the results  
 214 show that the presence of high-reactivity iron oxide nanomaterials improves adsorption efficiency.

215 **Table 3.** Codified variables and responses obtained for turbidity removal by NMAC and CAC.

Variables	Responses
-----------	-----------

Run	A: Dosage of adsorbent	B: Time of agitation	C: Rotation speed	D: Size of adsorbent	Removal	Efficiency (%)
	g	min	rpm	um	NMAC	CAC
1	-1	-1	-1	-1	93.69	83.77
2	-1	0	1	-1	98.84	79.93
3	0	-1	0	-1	94.33	74.29
4	1	-1	1	-1	96.33	80.65
5	-1	1	0	-1	96.93	65.96
6	0	0	-1	-1	97.94	87.6
7	0	1	1	-1	97.04	82.47
8	1	0	0	-1	95.37	73.24
9	1	1	-1	-1	98.17	89.8
10	0	0	0	-1	97.22	78.29
11	0	0	0	-1	96.34	78.04
12	1	-1	-1	-1	92.53	77.84
13	1	0	1	-1	97.98	83.78
14	-1	-1	0	-1	94.89	79.86
15	0	-1	1	-1	97.93	86.42
16	-1	-1	-1	1	84.54	87.31
17	-1	0	1	1	95.33	82.41
18	0	-1	0	1	88.33	81.72
19	1	-1	1	1	92.38	83.24
20	-1	1	0	1	92.54	82.03
21	0	0	-1	1	90.71	90.54
22	0	1	1	1	97.23	82.26
23	1	0	0	1	91.98	80.83
24	1	1	-1	1	93.33	92.03
25	0	0	0	1	91.83	83.42
26	0	0	0	1	92.18	82.99
27	1	-1	-1	1	86.02	86.34
28	1	0	1	1	95.11	90.68
29	-1	-1	0	1	87.07	84.71

216

217 3.3. Empirical model development for adsorption study

218 An empirical mathematical model had been generated through a method of steepest ascent and  
 219 multiple regression analysis of experimental data (Table 3). A predicted response (Y) for turbidity  
 220 removal efficiency of NMAC and CAC was expressed based on second-order polynomial equation  
 221 as in Eq (3) and Eq (4), respectively. In the equations, A B, C, and D are coded variables for dosage  
 222 of adsorbent, time of agitation, rotation speed, and size of adsorbent, respectively. In this study, D  
 223 (adsorbent size) is a two-level categorical factor that duplicated for every combination of main effect  
 224 factors (e.g. AABC, ABBC, ABCC). In an area with negligible quadratic effect, categorical factor  
 225 D=ABC was converted to AB, BD, and CD. BC in the given equation was not converted because it  
 226 has a 3-level quadratic effect. According to the given equations, the estimated response at the  
 227 stationary point (center of the system) for NMAC is 94.87; meanwhile, CAC is 82.03. Therefore, it  
 228 is an estimation that the performance of NMAC in removing turbidity in groundwater is higher than  
 229 CAC. The negative sign in the equations indicates antagonistic effects; meanwhile, the positive sign  
 230 indicated synergistic effects. Since the generated empirical equations (Eq. 3 and Eq. 4) are mixed in  
 231 a positive and negative sign, it shows that the stationary point is a saddle point (Myers *et al.*, 2016).  
 232 So, the strategy for improving turbidity removal efficiency in the saddle system is flexible (i.e.,  
 233 minimum and maximum range of each variable are considered in optimization process) and depend  
 234 on the nature of the response system.

235  $Y[NMAC(\%)] = +94.87 + 0.17A + 1.85B + 1.59C + 2.28D - 0.39A^2 - 1.82B^2 + 1.33C^2 -$   
 236  $0.31AC - 0.5AD - 1.11BC - 0.68BD - 0.94CD \dots\dots\dots$  Equation 3

237

238  $Y[CAC(\%)] = +82.03 + 2.36A - 0.27B - 1.26C + 1.80D - 4.29A^2 - 2.62B^2 + 7.27C^2 +$   
 239  $5.88AB + 1.26AD - 1.25BC - 1.82BD + 0.42CD \dots\dots\dots$  Equation 4

240 Table 4 shows the screening of designs based on the analysis of block for second-order models in the  
 241 form of analysis of variance (ANOVA) generated by Design Expert v.11. The p-values for NMAC  
 242 and CAC are less than 0.005 which indicates that the model terms are significant. The F-values are  
 243 compared to identify the fittest model. The highest F-value for NMAC and CAS are quadratic models  
 244 with 119.34 and 626.26, respectively. This is because of the larger F-value, and the smaller p-value,  
 245 which denotes the most significant of the corresponding coefficients (Shahmoradi *et al.*, 2018).

246 **Table 4.** Sequential model of sum squares for NMAC and CAC.

Types of adsorbents	Source	Sum of Squares	df	Mean Square	F-value	p-value
<b>NMAC</b>	Mean vs Total	5.385E+005	1	5.385E+005		
	Block vs Mean	3.19	2	1.59		
	Linear vs Block	484.88	4	121.22	52.89	< 0.0001
	2FI vs Linear	71	6	11.83	10.76	< 0.0001
	Quadratic vs 2FI	46.87	3	15.62	119.34	< 0.0001
	Cubic vs Quadratic	3.03	13	0.23	2.61	0.0135
	Residual	2.86	32	0.089		
	Total	5.391E+005	61	8837.14		
<b>CAC</b>	Mean vs Total	3.98E+05	1	3.98E+05		
	Block vs Mean	179.3	2	89.65		
	Linear vs Block	415.06	4	103.76	3.68	0.0104
	2FI vs Linear	701.16	6	116.86	7.01	< 0.0001
	Quadratic vs 2FI	749.61	3	249.87	626.26	< 0.0001
	Cubic vs Quadratic	6.85	13	0.5272	1.54	0.1619
	Residual	10.3	30	0.3434		
	Total	4.00E+05	59	6785.01		

248 The lack of fit test is carried out to compare the residual and the pure error. The ‘lack of fit F-value’  
 249 ( $F_0$ ) for NMAC and CAC (Table 5) are 1.22 and 0.8082, respectively, and their p-values are relatively  
 250 big. So, we accept the hypothesis that the models adequately describe the data. There are 41.06%  
 251 (NMAC) and 69.29% (CAC) chance that the ‘lack of fit F-value’ occurred due to noise. These results  
 252 imply that a lack of fit for these models was not significant relative to the pure error (Kumar *et al.*,  
 253 2018).

254

**Table 5.** Lack of fit test.

Types of adsorbents	Source	Sum of Squares	df	Mean Square	F-value	p-value
<b>NMAC</b>	Linear	122.87	46	2.67	24.07	< 0.0001
	2FI	51.88	40	1.30	11.68	0.0005
	Quadratic	5	37	0.14	1.22	0.4106
	Cubic	1.97	24	0.082	0.74	0.7329
	Pure Error	0.89	8	0.11		
<b>CAC</b>	Linear	1464.14	44	33.28	70.38	< 0.0001
	2FI	762.98	38	20.08	42.47	< 0.0001
	Quadratic	13.37	35	0.3821	0.8082	0.6929
	Cubic	6.52	22	0.2964	0.6268	0.8168
	Pure Error	3.78	8	0.4728		

255

### 256 3.3.1. Model Adequacy

257 Checking the adequacy of the model is critical to ensure that the empirical models have an adequate  
 258 approximation to the true system and to verify that the assumptions for square regression are at the  
 259 point of view (Tezcan *et al.*, 2015). The adequate empirical model must fulfill three residual  
 260 assumptions, consisting of a normal distribution, constant variance, and independence (Kumar *et al.*,  
 261 2018). Normal probability and studentized residual plots of the residuals of NMAC and CAC for  
 262 removal of turbidity (Figure 2 (a) and (b)) show that most of the points for residual plot concentrated

263 on the central portion of the data, these observations verify that the residuals are normal. Since the  
264 results indicate that there are no unusually large residuals, hence, a transformation of the response is  
265 not required, which is similar to the findings of Kumar *et al.*, (2018).

266

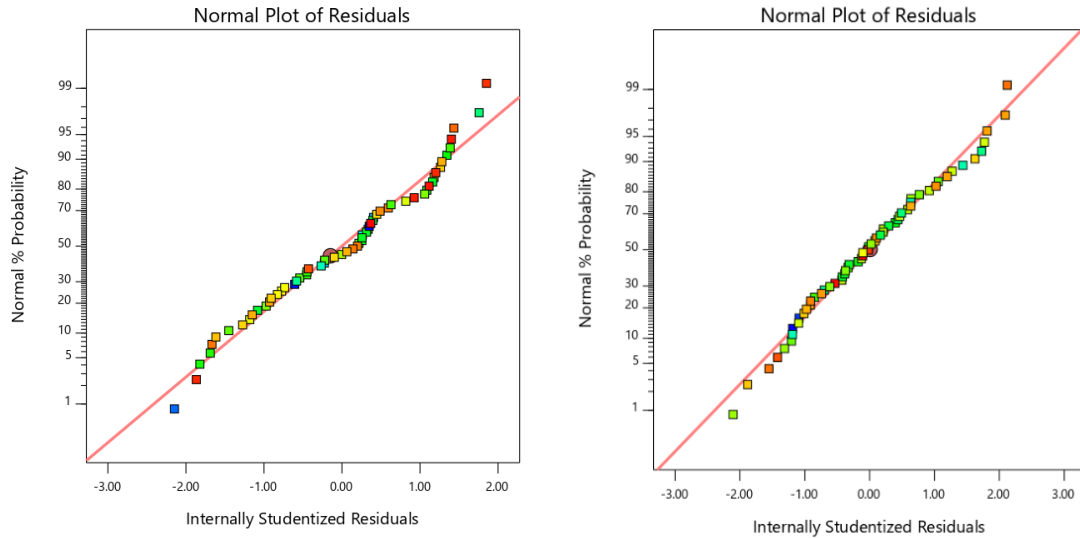
267

268

269

270

271



272

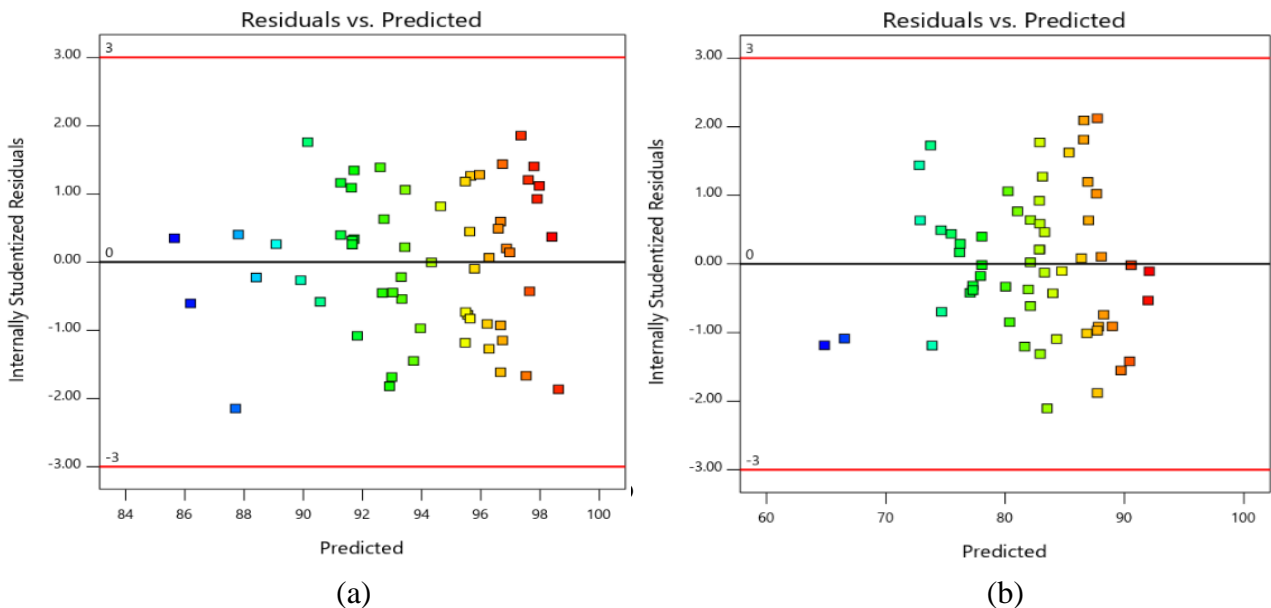
273 **Figure 2.** Studentized residual and normal probability plots for removal of turbidity by (a) NMAC  
274 and (b) CAC.

275

276 Moreover, Figure 3 (a) and (b) show that the residuals are scattered randomly with homoscedasticity.

277 The results reveal that the variance of residuals is constant for all values of  $y$  (Tezcan *et al.*, 2015).

278



279

280 **Figure 3.** Predicted turbidity removal and studentized residual plots for (a) NMAC and (b) CAC.

281

282 Another criterion to indicate the adequacy of the model is the assumption of the independent residual.

283 The assumption will be violated if there is a dependence between residuals which can be observed on

284 negative or positive pattern of the residual plot against time. Based on the observation, there are no

285 discernible pattern of graphs for both NMAC (Figure 4 (a)) and CAC (Figure 4 (b)). So, it is suggested

286 that the residuals are independent (Myers *et al.*, 2016).

287

288

289

290

291

292

293

294

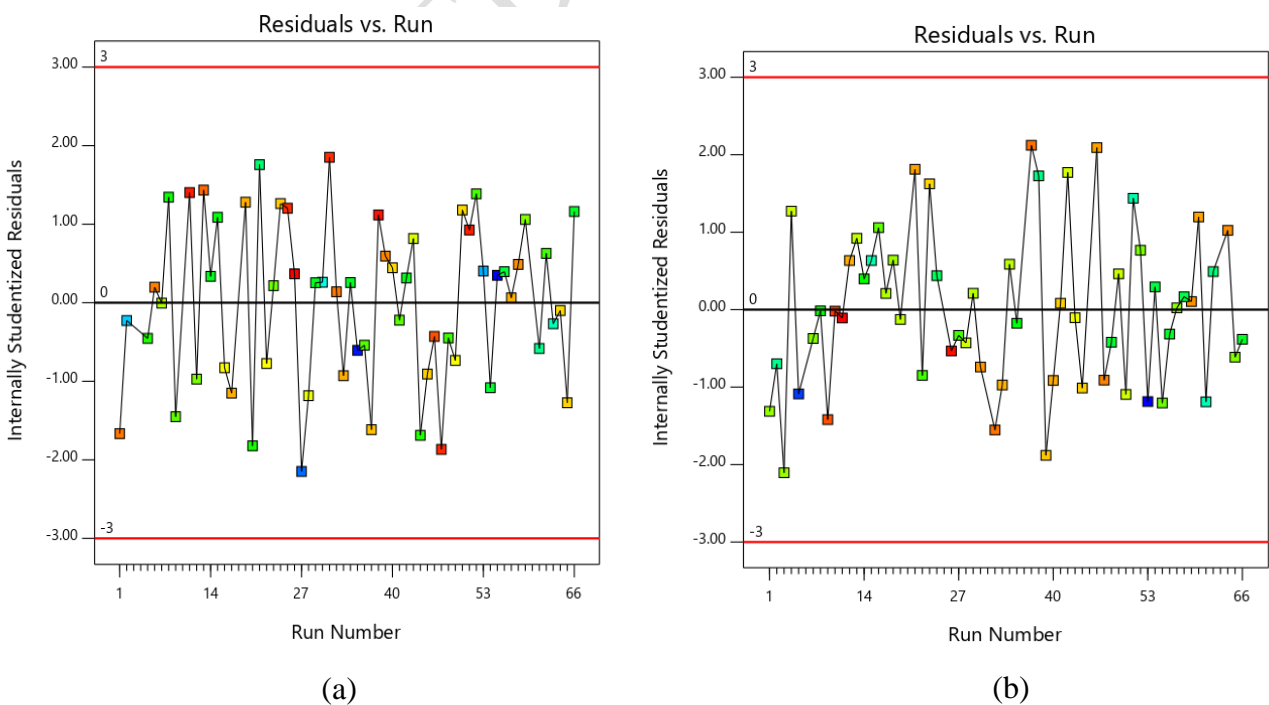
295

296

297

298

299



300 **Figure 4.** Studentized residual plots by run numbers for (a) nanomagnetic adsorbent composite  
301 (NMAC) and (b) commercial activated carbon (CAC).



302

303 *3.4. Analysis of variance (ANOVA)*

304 The Analysis of variance (ANOVA) (Table 6) investigates the correlation between variables and  
 305 processing parameters. The analysis reports a 95% confidence interval for model parameters, the  
 306 dosage of adsorbent, time of agitation, rotation speed, and dosage of adsorbent.

307 **Table 6.** Analysis of variance (ANOVA) for NMAC and CAC.

	Source	Sum of Squares	DF	Mean Square	F Value	Prob > F
<b>Types of adsorbents</b>						
<b>NMAC</b>	Block	3.19	2	1.59		
	Model	602.75	13	46.37	354.14	< 0.0001
	A	0.97	1	0.97	7.39	0.0093
	B	114.13	1	114.13	871.72	< 0.0001
	C	75.09	1	75.09	573.55	< 0.0001
	D	297.96	1	297.96	2275.79	< 0.0001
	A2	1.97	1	1.97	15.06	0.0003
	B2	31.34	1	31.34	239.37	< 0.0001
	C2	22.75	1	22.75	173.75	< 0.0001
	AB	0.17	1	0.17	1.32	0.2572
	AC	1.94	1	1.94	14.85	0.0004
	AD	8.13	1	8.13	62.08	< 0.0001
	BC	27.37	1	27.37	209.05	< 0.0001
	BD	16.25	1	16.25	124.09	< 0.0001
	CD	26.25	1	26.25	200.47	< 0.0001
	Residual	5.89	45	0.13		
	Lack of Fit	5	37	0.14	1.22	0.4106
Pure Error	0.89	8	0.11			
Cor Total	611.83	60				
<b>CAC</b>	Block	179.3	2	89.65		
	Model	1865.82	13	143.52	359.72	< 0.0001
	A	168.57	1	168.57	422.48	< 0.0001
	B	2.11	1	2.11	5.28	0.0264

C	46.77	1	46.77	117.21	< 0.0001
D	177.41	1	177.41	444.65	< 0.0001
A2	219.16	1	219.16	549.29	< 0.0001
B2	62.6	1	62.6	156.89	< 0.0001
C2	622.53	1	622.53	1560.28	< 0.0001
AB	757.16	1	757.16	1897.71	< 0.0001
AC	1.16	1	1.16	2.91	0.095
AD	49.03	1	49.03	122.88	< 0.0001
BC	32.36	1	32.36	81.11	< 0.0001
BD	98.75	1	98.75	247.51	< 0.0001
CD	5.26	1	5.26	13.18	0.0007
Residual	17.16	43	0.4		
Lack of Fit	13.37	35	0.38	0.81	0.6929
Pure Error	3.78	8	0.47		
Cor Total	2062.28	58			

308

309 However, there are non-significant terms (Table 6) for NMAC (AB; p-value > 0.05) and CAC (AC;  
310 p-value > 0.05). As a result, the identified terms were dropped in the empirical model resulting in the  
311 formation of reduced quadratic model for the process (Eq. 3 and Eq. 4). It is important to drop the  
312 non-significant terms as there are differences between full and reduced model in predicted error sum  
313 of squares (PRESS) and Adjusted R-Squared (Table 7). The reduced quadratic model in this study is  
314 in agreement with Shahmoradi *et al.*, (2018) findings that the generated empirical models is better  
315 satisfied after dropping non-significant terms. The analysis is considered to support the generated  
316 empirical models and are good because more than half of the terms in ANOVA are significant  
317 (Shahmoradi *et al.*, 2018).

318 **Table 7.** Comparison between full quadratic and reduced quadratic model for NMAC and CAC.

Sources	NMAC		CAC	
	Full quadratic model	Reduced quadratic model	Full quadratic model	Reduced quadratic model

<b>Std.Dev</b>	0.36	0.36	0.63	0.65
<b>Mean</b>	93.95	93.95	82.16	82.16
<b>CV</b>	0.39	0.39	0.77	0.79
<b>PRESS</b>	11.68	11.32	34.46	35.35
<b>R-Squared</b>	0.9903	0.9900	0.9909	0.9903
<b>Adj R-Squared</b>	0.9875	0.9874	0.9881	0.9876
<b>Pred R-Squared</b>	0.9808	0.9814	0.9817	0.9812
<b>Adeq Precision</b>	70.049	72.204	82.74	84.349

319

320

321

### 322 3.5. Effect of adsorption parameters

323 The perturbation plot is used to investigate changes in responses as each individual factor moves from  
324 the selected reference point while the other factors at the reference value are held constant. The  
325 reference point is the coded zero level in the middle of the design space. A steep slope in the results  
326 suggest the sensitivity of a response to a factor. As far as the slope was concerned, positive coefficient  
327 was pushed up while negative coefficient was pressed down (Anderson & Whitcomb, 2017). The  
328 studied factors include dosage of adsorbent (A), time of agitation (B), rotation speed (C), and size of  
329 adsorbent (D). The perturbation plots for NMAC with size of adsorbent  $< 45 \mu\text{m}$  and  $> 300 \mu\text{m}$  are  
330 represented in Figure 5 (a) and (b) respectively. The perturbation plot for NMAC (Figure 5 (a) and  
331 (b)) show that factor A (dosage of adsorbent) produces relatively flat line. So, it is suggested that  
332 dosage of adsorbent (A) was sensitive to turbidity removal efficiency but the lowest influence on  
333 removal process. Meanwhile the steepest curve of factor B (time of agitation) and C (rotation speed)  
334 indicate that turbidity removal efficient is sensitive to time and rotation speed. The research found  
335 that turbidity removal efficiency among different dosages of NMAC (0.02, 0.04, and 0.06 g) showed  
336 relatively small difference. This might be due to the presence of iron oxide nanomaterials on the

337 surface of adsorbent which improves activation of the pores. Besides, another reason is likely because  
338 of the process of separating NMAC from groundwater, which is aided by external magnetic field.  
339 The efficient separation process to separate NMAC regardless of the amount of dosage resulted in  
340 clean water without leaving any adsorbent residues in the groundwater sample. When compared to  
341 the perturbation plots for CAC with the size of adsorbent  $< 45 \mu\text{m}$  and  $> 300 \mu\text{m}$  in Figure 5 (c) and  
342 (d), respectively, factor B (time of agitation) shows relatively small effect as it moved from the  
343 reference point. Factor C (rotation speed) shows the steepest curve in both Figure (5 (c)) and (d).  
344 Hence, it indicates that turbidity removal is insensitive to time of agitation (B) but sensitive to rotation  
345 speed (C). The role of factor A (dosage of adsorbent) is dynamic between two ranges of adsorbent  
346 size. The turbidity removal efficiency is more sensitive to dosage of adsorbent with larger size ( $> 300$   
347  $\mu\text{m}$ ). Turbidity removal efficiency is relatively insensitive towards time of agitation, this might be  
348 due to rapid adsorption. Apart from that, separation efficiency is weak for CAC. Since CAC does not  
349 have magnetic properties, the separation of CAC by using filter paper might leave some adsorbent  
350 residues in the groundwater sample. Thus, even though the adsorption is well at the given time of  
351 agitation, the inefficient separation causes drawback on quality of treated groundwater.

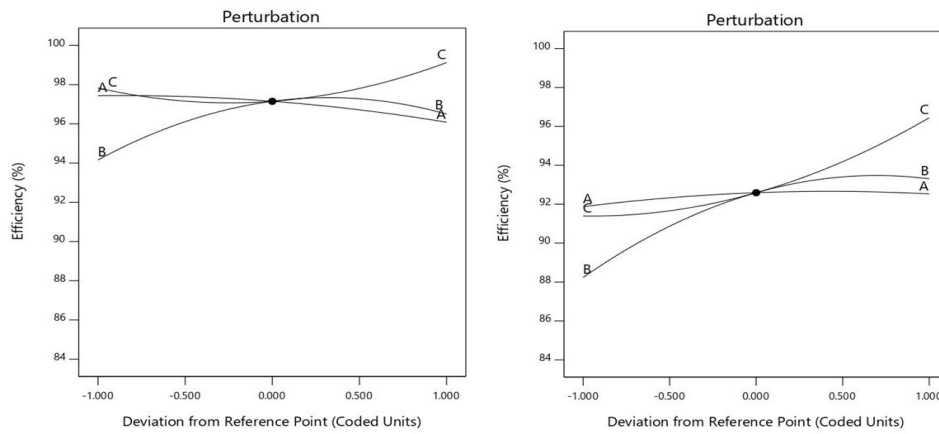
352

353

354

355

356



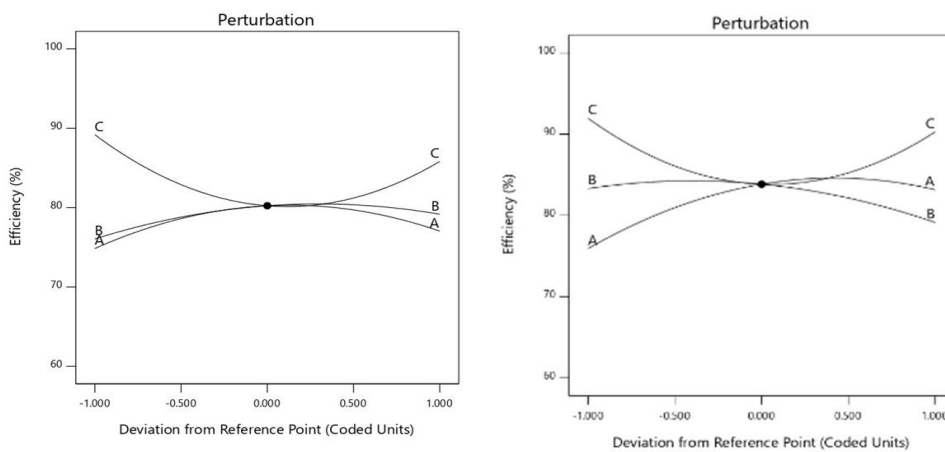
357

358

359

360

361



362

363

364

365

**Figure 4.** Perturbation plots for turbidity removal efficiency for (a) NMAC with size < 45  $\mu\text{m}$ , (b) NMAC with size > 300  $\mu\text{m}$ , (c) CAC with size < 45  $\mu\text{m}$ , and (d) CAC with size > 300  $\mu\text{m}$ .

366

### 3.5.1. Optimization

367

368

369

370

371

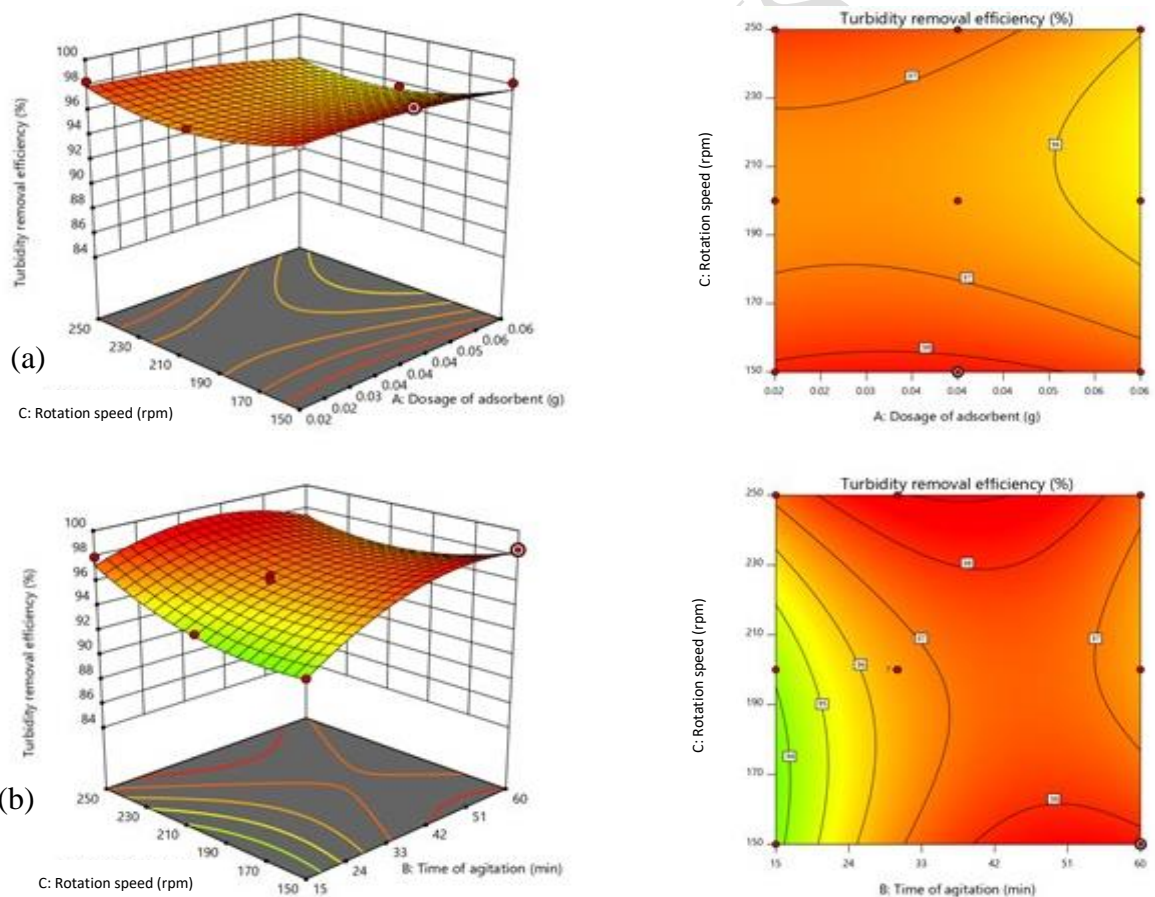
372

373

374

The empirical model generated graphs of 3D response surface and 2D contour plots to portray the interaction between independent and dependent variables. The significance of the interactions is indicated by elliptical shape, whereas the circular shape indicates insignificant interaction. The 3D response surface and contour plots (Figure 6 (a)) shows the interaction between dosage of adsorbent (A) and rotation speed (C) for NMAC. The increase in the dosage of adsorbent from 0.02 g to 0.04 g improves turbidity removal efficiency. The decline in turbidity removal efficiency occurred when the dosage of adsorbent is over 0.04 g, and there is no obvious effect when rotation speed is over 150 rpm. The turbidity removal efficiency decreased at a relatively high rotation speed as molecules in

375 turbid raw water and adsorbent are hastily colliding with each other and lead to detachment of loosely  
 376 bound impurities molecule (Latinwo *et al.*, 2019). The results shown in Figure 6 (b) indicates that the  
 377 optimum turbidity removal time by NMAC lies between 24 min to 33 min. Increment in time of  
 378 agitation may improve turbidity removal efficiency, but it does not show any obvious effect as  
 379 rotation speed increases. The rapid adsorption may occur due to diffusion control from the bulk of  
 380 the liquid phase to the unoccupied binding site at the surface of the adsorbent (Latinwo *et al.*, 2019).  
 381 In accordance with the present results, the previous study by Liang (2018) concurred that rapid  
 382 sorption of contaminants occurs at the initial rate and occupied sites of CoFe<sub>2</sub>O<sub>4</sub>/AC, resulting in the  
 383 sorption to decrease at a later stage.



394 **Figure 5.** 3D Response surface and 2D contour plots for speed of agitation and dosage of NMAC  
 395 for the interaction of: (a) dosage of adsorbent and rotation speed (AC) and (b) time of agitation and  
 396 rotation speed (BC).

397

398 Figure 7 (a) exhibits the relationship between the dosage of adsorbent and time of agitation on  
399 turbidity removal efficiency of CAC. The increment of the dosage of adsorbent along with time  
400 improves turbidity removal efficiency. However, the removal efficiency declined as the dosage of  
401 adsorbent exceeded 0.04 g, and the time of agitation was beyond 24 min to 33 min. Slow adsorption  
402 occurs at a later stage occur as a result of the smaller available site for adsorption (Sivaprakasam &  
403 Venugopal, 2019), and this limitation might occur because iron oxide nanomaterials are not present  
404 on the surface of CAC. Moreover, the interaction between time of agitation and rotation speed in  
405 Figure 7 (b) depicts that optimum turbidity removal efficiency lies in the range 24 to 33 min and 190  
406 rpm to 210 rpm. Turbidity that is due to solutes that reduce the surface tension of water can be easily  
407 taken up by the adsorbent (CAC). The high rate of a collision results in high adsorption. However,  
408 physical adsorption involves weak van der Waals force (Patterson, 2009). So, it is likely to affect  
409 turbidity removal efficiency during the later stages at rotation speed of above 210 rpm.

410

411

412

413

414

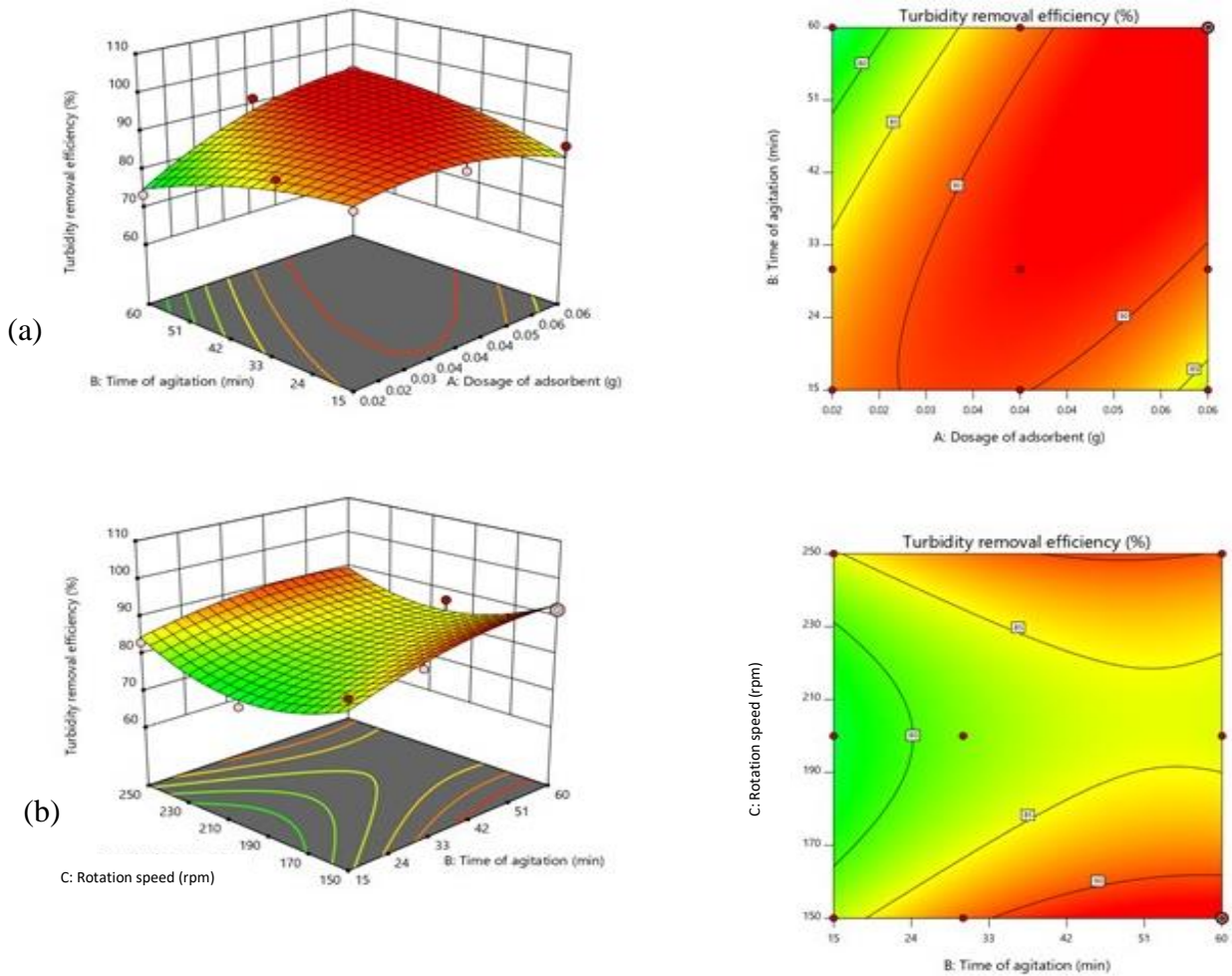
415

416

417

418

419



420 **Figure 6.** 3D Response surface and 2D contour plots for speed of agitation and dosage of CAC for  
 421 the interaction of (a) dosage of adsorbent and agitation time (AB) and (b) time of agitation and  
 422 rotation speed (BC).

423

424 *3.6. Verification of the predictive model*

425 The optimization experiment is conducted to identify optimum conditions for maximum turbidity  
 426 removal efficiency. Table 7 shows the generated optimum condition by Design Expert 11 and actual  
 427 results gathered for NMAC and CAC, respectively. The readings show that turbidity removal  
 428 efficiency by NMAC is 98.76% (0.40 NTU), whereas the performance of CAC is 84.84% (3.07  
 429 NTU). So, the treated groundwater complies with the Malaysia drinking water standard, which is  
 430 below 5 NTU. The results reveal that the actual value turbidity removal efficiency by NMAC is 0.26%  
 431 higher than the predicted value. Also, the actual value for turbidity removal efficiency by CAC is



432 0.21% higher than predicted value. Overall, the results indicated that the optimization parameters are  
433 reliable with no significant differences between predicted and actual results.

434

435 **Table 7.** Optimized parameters with predicted and actual value for turbidity removal efficiency by  
436 both NMAC and CAC.

Types of adsorbents	Condition	Turbidity removal efficiency (%)	Dosage of adsorbent (g)	Time of agitation (min)	Rotation speed (rpm)	Size of adsorbent ( $\mu\text{m}$ )
NMAC	Predicted	98.50	0.04	48	150	<45
	Actual	98.76	0.04	48	150	<45
CAC	Predicted	84.66	0.03	22	250	<45
	Actual	84.84	0.03	22	250	<45

437

#### 438 4.0. Conclusion

439 Nanomagnetic adsorbent composite (NMAC) was used for adsorption study for turbidity removal of  
440 groundwater and commercial activated carbon (CAC) as a standard reference for comparison. RSM  
441 was adopted in the study to optimize turbidity removal efficiency factors. Model adequacy analysis  
442 revealed that the generated quadratic model fits the experiment carried out. From the derived  
443 quadratic model for turbidity removal efficiency and analysis of variance, 0.93% of adsorbent dosage  
444 (NMAC) and 2.64% of agitation time for CAC were considered as high compared to other extreme  
445 values in Table 6 ( $>0.0000001$ ). Although the p-values of main effects (adsorbent dosage (NMAC)  
446 and agitation time (CAC)) are less than 0.05, the obtained values were closer to calculated null  
447 hypothesis compared to other reported main effects (Table 6). . The results show the crucial role of  
448 iron oxide nanomaterial adsorbent composite in turbidity removal from raw water. The optimum  
449 NMAC process parameters were 0.04 g adsorbent dose, 45  $\mu\text{m}$  adsorbent size, 48 min agitation at  
450 150 rpm rotation speed. The test showed that the optimal parameters were accurate and that NMAC's  
451 performance was 14% higher than CAC for optimal turbidity removal efficiency. Consequently, for

452 subsequent stage of scaling up, the created empirical model from a 3k factorial design is useful and  
453 that NMAC is a competitive adsorbent to treat water efficiently compared to CAC.

#### 454 **5.0. Acknowledgment**

455 The authors acknowledge financial support from Universiti Malaysia Kelantan Research Fund  
456 (R/PRO/A07.00/01397A/008/2021/00975) and (R/SGJP/A07.00/01397A/005/2018/0057).

#### 457 **6.0. References**

458 Anderson M. J. and Whitcomb, P. J. (2017), *RSM Simplified*. CRC Press (2th.)

459 Ayob, N. A. F. C., & Musa, S. (2022). Frequency Analysis on Groundwater Consumption and Water  
460 Billed to the Community in Kelantan. In IOP Conference Series: Earth and Environmental  
461 Science (Vol. 1022, No. 1, p. 012073). IOP Publishing.

462 Basrur D., and Ishwara B. J. (2019), An investigation on the characterization of activated carbon  
463 from areca leaves and their adsorption nature towards different dyes, *Global NEST Journal*,  
464 **21**(2), 124–130.

465 Crini G., Lichtfouse E., Wilson L. D. and Morin N. (2018), Conventional and non-conventional  
466 adsorbents for wastewater treatment, *Environmental Chemistry Letters*, **17**(1), 195-213.

467 Hazimah H.H., Mohamad R., Nurhidayu S., Zulfa, H. A. and Faradiella, M. K. (2019),  
468 Hydrogeochemistry investigation on groundwater in Kuala Langat, Banting, Selangor, *Bulletin*  
469 *of the Geological Society of Malaysia*, **67**, 127-134.

470 Hidayu A. R., Mohamad N. F., Matali S. and Sharifah A. S. A. K. (2013), Characterization of  
471 activated carbon prepared from oil palm empty fruit bunch using BET and FT-IR techniques,  
472 *Procedia Engineering*, **68**, 379-384.

473 Huda, A., Palsan, S. A., & ZulAriff, A. L. (2020). A preliminary study of local behaviour,

474 perceptions & willingness to pay towards better water. In IOP Conference Series:  
475 Earth and Environmental Science (pp. 1-10).

476 Awang, H., Abdullah, P. S., Wen, L., Ling, H. Y., Barasarathi, J., & Azmin, S. N. H. M. (2022). Raw  
477 Water Treatment from Selected Areas In Kelantan Using Coconut Shell Derived Nanomagnetic  
478 Adsorbent Composite (CS-NMAC). *Journal of Sustainability Science and Management*, 17(2),  
479 77-90.

480 Karthikeyan S., Sivakumar P. and Palanisamy P. N. (2008), Novel Activated Carbons from  
481 Agricultural Wastes and their Characterization, *E-Journal of Chemistry*, 5, 409-426.

482 Kumar S., Meena H., Chakraborty S. and Meikap B. C. (2018), Application of response surface  
483 methodology (RSM) for optimization of leaching parameters for ash reduction from low-grade  
484 coal, *International Journal of Mining Science and Technology*, 28(4), 621-629.

485 Latinwo G. K., Alade A. O., Agarry S. E. and Dada E. O. (2019), Process Optimization and Modeling  
486 the Adsorption of Polycyclic Aromatic-Congo Red Dye onto Delonix regia Pod-Derived  
487 Activated Carbon, *Polycyclic Aromatic Compounds*, 3(1), 38-45.

488 Liang Y., He Y., Wang T. and Lei L. (2019), Adsorptive removal of gentian violet from aqueous  
489 solution using  $\text{CoFe}_2\text{O}_4$  / activated carbon magnetic composite, *Journal of Water Process*  
490 *Engineering*, 27, 77-88.

491 Liu Z., Wei H., Li A. and Yang H. (2018), Enhanced coagulation of low-turbidity micro-polluted  
492 surface water: Properties and optimization, *Journal of Environmental Management*, 233, 739-  
493 747.

494 Meng P., Fang X., Maimaiti A., Yu G. and Deng S. (2019), Efficient removal of perfluorinated  
495 compounds from water using a regenerable magnetic activated carbon, *Chemosphere*, **224**, 187-  
496 194.

497 Milne T. A., Chum H. L., Agblevor F. A. and Johnson D. K. (1992), “Standardized Analytical  
498 Methods’ Biomass & Bioenergy, *Proceedings of International Energy Agency Bioenergy*  
499 *Agreement Seminar*, **2**(1–6), 341-366.

500 Ministry of Health Malaysia. (2014), Drinking Water Quality Standards and Frequency of  
501 Monitoring. Retrieved December 7, 2019, from [http://kmam.moh.gov.my/public-user/drinking-](http://kmam.moh.gov.my/public-user/drinking-water-quality-standard.html)  
502 [water-quality-standard.html](http://kmam.moh.gov.my/public-user/drinking-water-quality-standard.html)

503 Mohd F. F. R. and Noorazuan M. (2018), Perubahan Kualiti Air Bawah Tanah di Negeri Kelantan  
504 Pada Tahun 2010 Hingga 2012, *Jurnal Wacana Sarjana*, **2**(2), 1-10.

505 Muoio R., Caretti C., Rossi L., Santianni D. and Lubello C. (2020), International Journal of Hygiene  
506 and Water safety plans and risk assessment: A novel procedure applied to treated water turbidity  
507 and gastrointestinal diseases, *International Journal of Hygiene and Environmental Health*, **223**  
508 (1), 281-288.

509 Myers R. H., Montgomery D. C. and Anderson C. C. M. (2016), Response Surface Methodology  
510 (4th.), New Jersey: John Wiley & Sons, Inc.

511 Park W., Jeong S., Im S. and Jang A. (2020), High turbidity water treatment by ceramic  
512 microfiltration membrane: Fouling identification and process optimization, *Environmental*  
513 *Technology & Innovation*, **17**, 100578.

514 Patterson H. B. W. (2009), Adsorption, In *Bleaching and Purifying Fats and Oils Theory and Practice*  
515 Elsevier Inc.

- 516 Santhosh C., Malathi A., Dhaneshvar E., Bhatnagar A., Grace A. N. and Madhavan J. (2019), *Chapter*  
517 *16 - Iron Oxide Nanomaterials for Water Purification. Nanoscale Materials in Water*  
518 *Purification*. Elsevier Inc.
- 519 Shahmoradi B., Yavari S., Zandsalimi Y., Shivaraju H. P., Negahdari M., Maleki A., McKay G.,  
520 Radheshyam R.P. and Lee S. M. (2018), Optimization of solar degradation efficiency of bio-  
521 composting leachate using Nd: ZnO nanoparticles, *Journal of Photochemistry and Photobiology*  
522 *A: Chemistry*, **356**, (1), 201-211.
- 523 Sivaprakasam A. and Venugopal T. (2019), Modelling the removal of lead from synthetic  
524 contaminated water by activated carbon from biomass of *Diplocyclos Palmatus* by RSM, *Global*  
525 *NEST Journal*, **21**(3), 319–327.
- 526 Sun H., Yang B. and Li A. (2019), Biomass derived porous carbon for efficient capture of carbon  
527 dioxide, organic contaminants and volatile iodine with exceptionally high uptake, *Chemical*  
528 *Engineering Journal*, **372**(4), 65-73.
- 529 Tancredi P., Veiga L. S., Garate O. and Ybarra G. (2019), Magnetophoretic mobility of iron oxide  
530 nanoparticles stabilized by small carboxylate ligands, *Colloids and Surfaces A*, **579**(5), 123664.
- 531 Tezcan Un, U., Ates F., Erginel N., Ozcan O. and Oduncu E. (2015), Adsorption of Disperse Orange  
532 30 dye onto activated carbon derived from Holm Oak (*Quercus Ilex*) acorns: A 3k factorial  
533 design and analysis, *Journal of Environmental Management*, **155**, 89-96.
- 534 Wannahari R., Sannasi P., Nordin M. F. M. and Mukhtar H. (2018) Sugarcane Bagasse Derived Nano  
535 Magnetic Adsorbent Composite (Scb-Nmac) for Removal of Cu<sup>2+</sup> From Aqueous Solution,  
536 *ARPN Journal of Engineering and Applied Sciences*, **13**(1), 1-9.

- 537 World Health Organization (WHO). 2022. Groundwater, invisible but vital to health. Retrieved July  
538 7, 2022, from [https://www.who.int/news-room/feature-stories/detail/world-water-day-2022-](https://www.who.int/news-room/feature-stories/detail/world-water-day-2022-groundwater-invisible-but-vital-to-health)  
539 [groundwater-invisible-but-vital-to-health](https://www.who.int/news-room/feature-stories/detail/world-water-day-2022-groundwater-invisible-but-vital-to-health).
- 540 Yong C. Z., Denys P. H., Pearson C. F. and Pearson C. F. (2018), Groundwater extraction-induced  
541 land subsidence: a geodetic strain rate study in Kelantan, Malaysia strain rate study in Kelantan,  
542 Malaysia, *Journal of Spatial Science*, **8596**, 1-12.
- 543 Zainol NFM, Zainuddin AH, Looi LJ, Aris AZ, Isa NM, Sefie A, Ku Yusof KMK. (2021). Spatial  
544 Analysis of Groundwater Hydrochemistry through Integrated Multivariate Analysis: A Case  
545 Study in the Urbanized Langat Basin, Malaysia. *Int J Environ Res Public Health*.  
546 27;18(11):5733.
- 547 Zhu Z., Huang C. P., Zhu Y., Wei W. and Qin H. (2018), A hierarchical porous adsorbent of nano-  $\alpha$   
548  $-\text{Fe}_2\text{O}_3 / \text{Fe}_3\text{O}_4$  on bamboo biochar (HPA-Fe / C-B) for the removal of phosphate from water,  
549 *Journal of Water Process Engineering*, **25**, (4), 96-104.
- 550 Zulkania A., F G. H. and Rezki A. S. (2018), The potential of activated carbon derived from bio-char  
551 waste of bio-oil pyrolysis as adsorbent, *MATEC*, *01029*, 1-6.

552

553